

# FINITE ELEMENT MODEL UPDATING OF THE GARTEUR SM-AG19 STRUCTURE

Carole Thonon, Jean-Claude Golinval

*Université de Liège, LTAS - Vibrations et identification des structures,  
Chemin des chevreuils, 1 (Bât. B52/3), B-4000 Liège, Belgium*

**SUMMARY:** This paper reports the procedure followed by the "LTAS-Vibrations et Identification des Structures" research group to generate a low order finite element (F.E.) model of the GARTEUR SM-AG19 structure proposed as benchmark in the framework of the European COST Action F3 in structural dynamics. The model is made of beam elements, local inertia and rigid body elements. First, the correlation of the experimental data with the results of the F.E. model shows different levels of discrepancies. To perform local error detection, the size of the measured mode shape vectors is first expanded to the size of the F.E. eigenvectors. Model error localisation is based on the computation of residual strain energy due to errors in the constitutive equations. Updating parameters are then selected using eigenvalue sensitivity and local error analyses. The error localisation procedure is followed by the updating process in order to improve the accuracy of the FE models. The quality of the results is assessed in terms of accuracy of the response prediction to structural modifications.

**KEYWORDS:** Model Updating, Error Localisation.

## INTRODUCTION

The GARTEUR<sup>1</sup> SM-AG19 structure was proposed as benchmark for model updating methods in the framework of the European COST<sup>2</sup> Action F3 in structural dynamics. Experimental data were provided by the University of Manchester (UK) and by DLR (German Aerospace Establishment in Göttingen, Germany) [5]. New measurements on the original GARTEUR testbed and on a modified structure were also provided to the COST F3 participants by the Imperial College of Science, Technology and Medicine in London (UK) and by the University of Wales Swansea (UK). The benchmark consists first to generate and to update a F.E. model in the active frequency range from 0 to 65 Hz. Afterwards, the updated model is used :

- (1) to predict the eigenfrequencies and modes beyond the active frequency range;
- (2) to predict frequency response functions obtained from other loading conditions;
- (3) to predict modal data and/or FRF's of a modified structure.

---

<sup>1</sup>Group for **A**eronautical **R**esearch and **T**echnology in **E**urope

<sup>2</sup>Cooperation in the field of **S**cientific and **T**echnical Research

Only the works related to items 1 and 3 are reported in this paper.

The local error detection method presented hereafter is formulated from the application of variational principles commonly used for structural analysis by the F.E. method. When performing vibration measurements and modal analysis, one obtains displacement fields (i.e. experimental eigenvectors) to which can be associated "experimental" stress fields. However, these fields of "experimental" stresses that are deduced from the expansion of the measured eigenvectors and the fields of analytical strains can be considered as independent fields in the sense that they do not *a priori* verify the constitutive equations. The use of a general variational principle allows to release constraints between these two fields. Thus the variation on the independent fields restores the criterion to be minimised in order to perform a physically-based expansion technique of experimental eigenvectors.

## MODEL ERROR LOCALISATION IN STRUCTURAL DYNAMICS

Let us consider a structure and its associated finite element (F.E.) model and let us denote by  $\mathbf{u}$  the analytical (calculated) displacement vector and by  $\mathbf{v}$  the experimental displacement vector corresponding to the same resonance frequency. As only a subset of the analytical co-ordinates are measured, only partition  $\mathbf{v}_2 = \bar{\mathbf{v}}$  of the experimental vector  $\mathbf{v}$  is known.

As vectors  $\mathbf{u}$  and  $\mathbf{v}$  result from two different sources, they are first assumed to be independent fields. For the purpose of "test / F.E. model results" reconciliation, a general Hamilton's principle [3] can be stated in the form of a variational problem operating on the field variables of the continuous system. It has been shown in [1] that if vectors  $\mathbf{u}$  and  $\mathbf{v}$  *a priori* verify the following equations :

$$a \text{ priori conditions} \quad \begin{cases} \mathbf{K} \mathbf{u} - \bar{\omega}^2 \mathbf{M} \mathbf{v} = 0 & (a) \\ \mathbf{v}_2 = \bar{\mathbf{v}} & (b) \end{cases} \quad (1)$$

then the natural conditions of the Fraeijs de Veubeke's two-field principle are :

$$\text{natural conditions} \quad \begin{cases} \mathbf{K} (\mathbf{u} - \mathbf{v}) = 0 & (a) \\ \mathbf{u}_2 = \bar{\mathbf{v}} & (b) \end{cases} \quad (2)$$

where  $\bar{\omega}$  denotes the experimental frequency and  $\mathbf{M}, \mathbf{K}$  are the mass and stiffness matrices of the model.

The *a priori* conditions Eqn 1 require that the analytical/experimental displacement vectors satisfy the structural equilibrium equation and that the partition  $\mathbf{v}_2$  of the expanded vector matches the measured co-ordinates. The first natural condition Eqn 2-(a) restores the compatibility condition (i.e.  $\mathbf{v} = \mathbf{u}$ ) as it requires that the force vector associated with the experimental displacement vector  $\mathbf{v}$  becomes equal to the force vector associated with the analytical displacement vector  $\mathbf{u}$ . The second natural condition Eqn 2-(b) takes care of the best possible enforcement of the measured degrees of freedom by the corresponding components of the analytical mode shape vector.

The fulfilment of the natural conditions Eqn 2 according to the *a priori* conditions Eqn 1 results in minimising the following norms

$$\| \mathbf{K} (\mathbf{u} - \mathbf{v}) \| \quad \text{and} \quad \| \mathbf{u}_2 - \bar{\mathbf{v}} \| \quad (3)$$

The problem of " test / F.E. model results " reconciliation may be rewritten in terms of the following constrained optimisation problem :

$$\begin{aligned} \min_{\mathbf{u}} \quad & (\mathbf{u} - \mathbf{v})^T \mathbf{K} (\mathbf{u} - \mathbf{v}) + \alpha (\mathbf{u}_2 - \bar{\mathbf{v}})^T \mathbf{K}_R (\mathbf{u}_2 - \bar{\mathbf{v}}) \\ \text{subject to} \quad & \mathbf{K} \mathbf{u} = \bar{\omega}^2 \mathbf{M} \mathbf{v} \end{aligned} \quad (4)$$

where  $\alpha$  is a weighting coefficient that may be interpreted as a parameter of confidence in the measured data and  $\mathbf{K}_R$  is the reduced stiffness matrix at the measured co-ordinates.

The objective function in Eqn 4 may be interpreted as the search for the minimum of the residual strain energy between the analytical and the experimental modes.

If the experimental modes are assumed to be a linear combination of the analytical modes of the initial F.E. model, the solution of the expansion problem defined by Eqn 4 is straightforward and is known as the Minimisation of Errors on Constitutive Equations (MECE) ([1], [2]). Different methods for the expansion of the measured mode shapes to the full set of degrees of freedom of the model are studied in details in reference [2]. It has been shown in [2] that the System Equivalent Reduction Expansion Process (SEREP) [4] may be regarded as a simplified MECE solution.

### MECE-based Error Localisation

Error localisation methods aim to detect the elements in the F.E. model that are responsible for the discrepancy between analytical results and experimental data. Such methods can be used both for model updating and for failure detection on actual structures. The quality of the localisation depends strongly on the quality of the expansion process.

The MECE error localisation indicator consists in evaluating the residual energy associated with each mode shape vector at a local level (element-by-element or substructure-by-substructure) i.e.

$$E_{(k)}^s = \left( \mathbf{u}_{(k)}^s - \mathbf{v}_{(k)}^s \right)^T \mathbf{K}_s \left( \mathbf{u}_{(k)}^s - \mathbf{v}_{(k)}^s \right) \quad (5)$$

where subscript  $(k)$  refers to the  $k$ th mode shape vector and  $s$  denotes the  $s$ th element or substructure.

## APPLICATION TO THE GARTEUR SM-AG19 STRUCTURE

The model error localisation procedure described above was applied to the example of the GARTEUR SM-AG19 structure proposed by M. Link (University of Kassel, Germany) as benchmark in the framework of the European COST F3 Action in structural dynamics. A detailed description of the proposed benchmark is available in reference [5]. Some preliminary results are presented here using the new test data provided by M. Friswell (University of Wales Swansea, UK).

### The beam F.E. model

The F.E. model of the GARTEUR SM-AG19 structure shown in Fig. 1-(b) was generated using the commercial finite element code SAMCEF [6]. It consists of 62 beam elements with 468 degrees of freedom. The modelling assumptions are :

- the fuselage, the wings, the tail and the drums are modelled using Euler-Bernoulli beam elements;
- the additional masses at the tips of the drums are modelled using concentrated masses and inertia;
- rigid body elements are used to reproduce the exact location of the sensors;
- the connections between the fuselage and the wings and between the fuselage and the tail are modelled using beam elements for which equivalent area moments of inertia were roughly estimated to take into account the stiffening effect of the junctions.

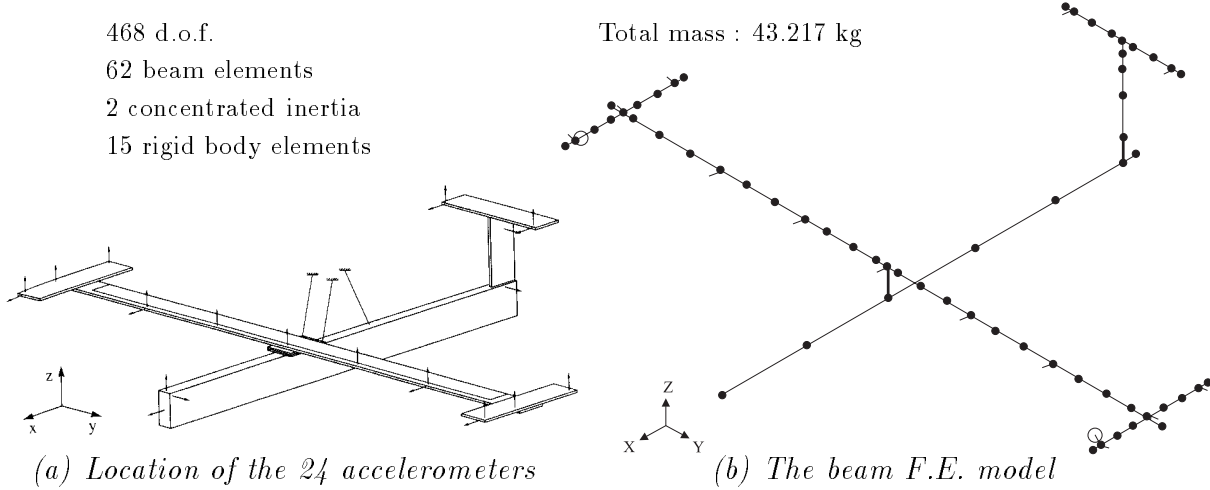


Fig. 1: The GARTEUR SM-AG19 structure

Table 1: Location of the elements in the model

Element n°	Location in the model
1 - 6	Fuselage
7 - 17	Right wing
18	Connection element on the right wing
19	Connection element on the left wing
20 - 30	Left wing
31 - 33	Horizontal tailplane (right side)
34	Connection element on the horizontal tailplane (right side)
35	Connection element on the horizontal tailplane (left side)
36 - 38	Horizontal tailplane (left side)
39 - 41	Vertical tail
42	Connection element on the vertical tail
43	Fuselage/tail connection element
44	Fuselage/wings connection element
45 - 52	Right drum
53	Connection element between the right drum and the wing
54 - 61	Left drum
62	Connection element between the left drum and the wing

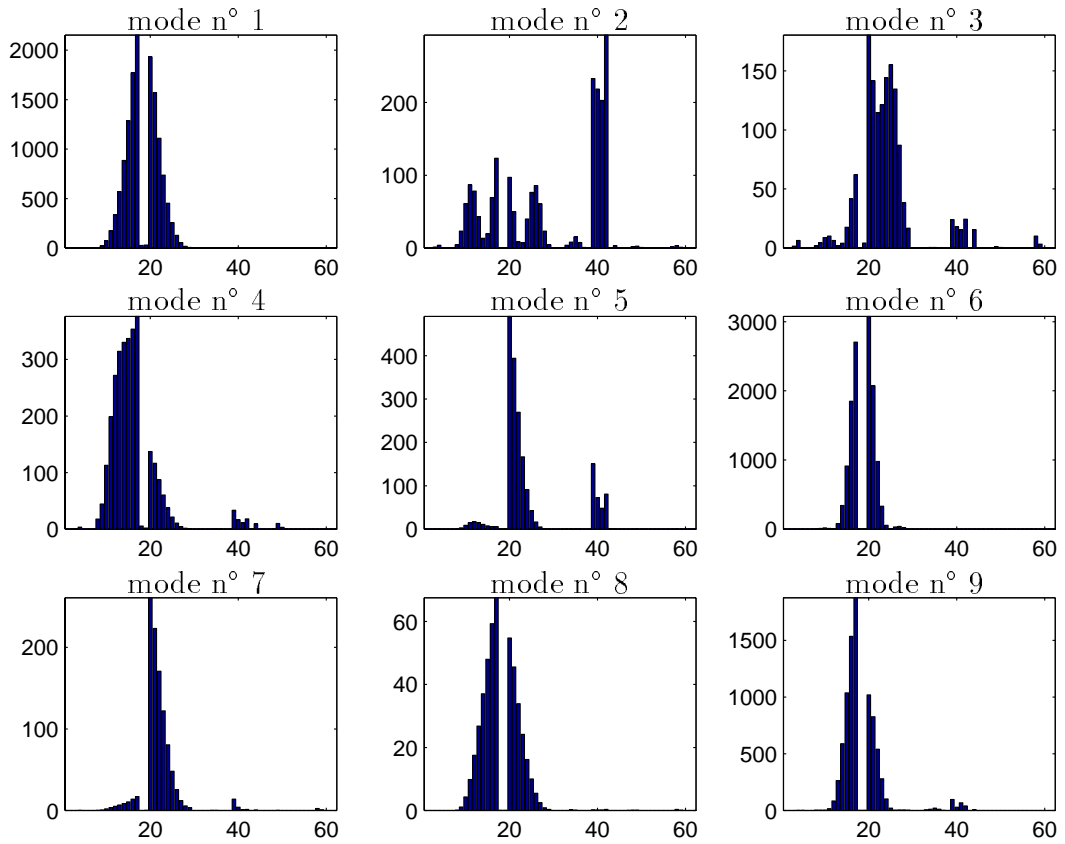
The degree of correlation between the predicted results from the initial F.E. model and the experimental data is given in Fig. 4-(a) in terms of the Modal Assurance Criterion (MAC) matrix and in Table 3-(a) in terms of resonance frequency deviations. In Table 3, the average MAC value and the average frequency deviation are defined as follows :

$$\overline{MAC} = \sum_{i=1}^9 \frac{MAC_i}{9} \quad \text{and} \quad \overline{\frac{|df|}{f}} = 100 \sum_{i=1}^9 \frac{|f_i - f_i^{exp}|}{9 f_i^{exp}} \quad (6)$$

An inversion is observed in the pairing of modes n° 5 and 6 and modes n° 9 and 10 between the analytical and the experimental results (Fig. 4-(a)). The deviations between the initial F.E. model results and the experimental results can be assigned to the modelling of joints and interconnections which remains a difficult task. As most of the model uncertainties lies in the modelling of the joints (wings/fuselage, tail/fuselage, horizontal/vertical tails), the area moments of inertia of the connecting beam elements were first chosen as parameters for a pre-updating of the model (parameters n° 9, 10, 12-14, 17-22 in Table 2). To enhance the quality of the initial F.E. model i.e. to pair all the modes in the frequency range of interest, a first correction was performed using only this first set of parameters.

### Localisation of Errors in the F.E. Model

The results of the error localisation procedure based on the MECE method are shown in Fig. 2 for the pre-updated model. In this particular example, only the modes that correlate well between the model and the measured data were used for expansion. Dominant modelling errors are identified on the wings and on the vertical tail as shown in Fig. 2. An asymmetry between the right and the left wings is observed mainly for modes n° 3, 4, 5 and 7.



(abscissa : element number referenced in Table 1.)

Fig. 2: Distribution of the strain residual energy

## Selection of Updating Parameters

The parameterisation of the F.E. model is given by

$$\mathbf{M} = \mathbf{M}_0 + \sum_{j=1}^{n_p} p_j \frac{\partial \mathbf{M}_j}{\partial p_j} \quad (7)$$

and

$$\mathbf{K} = \mathbf{K}_0 + \sum_{j=1}^{n_p} p_j \frac{\partial \mathbf{K}_j}{\partial p_j} \quad (8)$$

where  $\mathbf{M}_j$ ,  $\mathbf{K}_j$  are the mass and stiffness matrices of the  $j$ th element substructure and the coefficients  $p_j$ , ( $j = 1, \dots, n_p$ ) are the relative variations on physical parameters such as Young's modulus, area moments of inertia of the beams, mass density, etc.

The eigenvalue sensitivities are directly calculated from

$$\frac{\partial \omega_i^2}{\partial p_j} = \frac{\mathbf{u}_{(i)}^T (\mathbf{K}^* - \omega_i^2 \mathbf{M}^*) \mathbf{u}_{(i)}}{\mathbf{u}_{(i)}^T \mathbf{M} \mathbf{u}_{(i)}} \quad (9)$$

with

$$\mathbf{K}^* = \frac{\partial \mathbf{K}}{\partial p_j} \quad \text{and} \quad \mathbf{M}^* = \frac{\partial \mathbf{M}}{\partial p_j} \quad (10)$$

where  $\omega_i$  and  $\mathbf{u}_{(i)}$  denote the  $i$ th eigenvalue and eigenvector of the F.E. model. Note that the sensitivities shown in Fig. 3 are normalised by dividing Eqn 9 by  $\omega_i^2$ .

A set of 22 parameters were investigated in the sensitivity analysis for the 9 elastic modes in the active frequency range. From the results of Fig. 3 and from the localisation of residual strain energy (Fig. 2), a second set of local design parameters was chosen. Only seven parameters with high sensitivity values and relative independence were finally retained (parameters n° 3-8 and 15 of Table 2).

## Model Updating

The updating procedure was performed within the task manager and optimisation program BOSS-QUATTRO [6]. The objective function to be minimised is defined as follows :

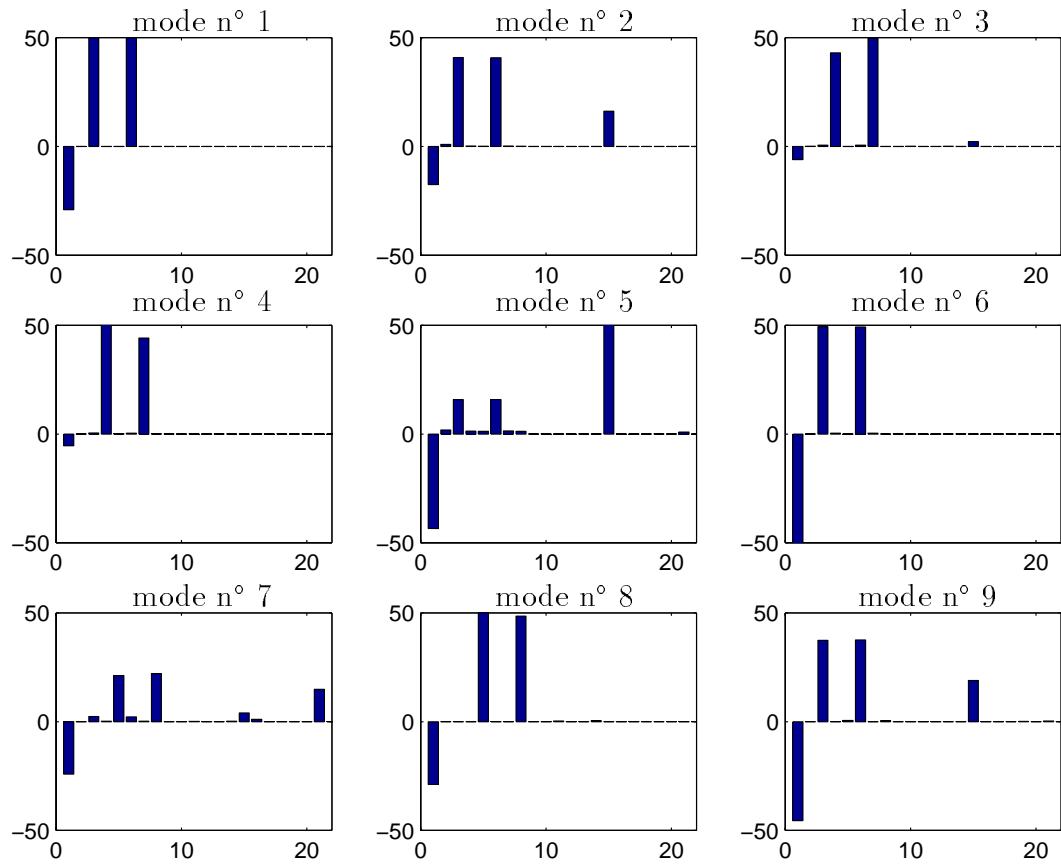
$$\frac{1}{2} \left( \sum_{i=1}^{10} \frac{(1 - MAC_i)}{10} + \sum_{i=1}^{10} \frac{1}{10} \frac{|f_i - f_i^{exp}|}{f_i^{exp}} \right) \quad (11)$$

where  $MAC_i$  refers to the paired MAC value corresponding to the  $i$ th experimental mode.

As the resonance frequency associated with mode n° 10 is very close to the active frequency range, it was decided to perform the model updating using the first ten modes to avoid pairing problems.

The optimisation solver follows the Method of Diagonal Quadratic Approximation (MDQA) in which the Hessians of the sequential quadratic problems are approximated by diagonal matrices. This method is known to be often a good compromise between the convergence order and the computational cost.

The MAC matrix between the analytical and the experimental modes of the updated F.E. model is shown in Fig. 4-(b) and the corresponding resonance frequency deviations are



(abscissa : parameter number referenced in Table 2)

Fig. 3: Eigenvalue sensitivity analysis

listed in Table 3. Note that the largest deviation (of 5.13 %) is observed for the first mode despite an excellent value of the corresponding MAC (0.9799). This deviation may be assigned to the lack of accuracy in the definition of the additional masses on the wing tips and of the viscoelastic layer. In this work, the additional masses were assumed to be known exactly and were not chosen as updating parameters. Table 3 and Fig. 4 show that the considered model is not suitable to well predict modal data beyond the active frequency range i.e. for modes n° 11 to 14.

### Prediction of Modal Data of Modified Structures

Two structural modifications are considered here, namely a mass added to the tail (modification n° 1) and a mass added to the wing tips (modification n° 2). The natural frequencies of the structure with these modifications show significant changes. For the first modification, the mode order has changed and interactions between some modes have appeared. The prediction of the modal data of the GARTEUR structure with each of its modifications and using the updated model is reported in terms of natural frequency deviations in Table 4 and in terms of MAC values in Fig. 5. The predicted results using the updated F.E. model are found to be in good agreement with the experimental data.

Table 2: List of parameters

N°	Parameter	Correction (%)	Location	Element n°
1	$\rho$	0	density of the wings	7 - 18
Fuselage				1-6
2	$I_{XX}$	0	torsional area moment of inertia	
Right wing				7-17
3	$I_{XX}$	10.5	bending area moment of inertia about x-axis	
4	$I_{YY}$	28.3	torsional area moment of inertia	
5	$I_{ZZ}$	5.5	bending area moment of inertia about z-axis	
Left wing				20-30
6	$I_{XX}$	1	bending area moment of inertia about x-axis	
7	$I_{YY}$	25.8	torsional area moment of inertia	
8	$I_{ZZ}$	4.2	bending area moment of inertia about z-axis	
Connection element on the right wing				18
9	$I_{XX}$	0	bending area moment of inertia about x-axis	
10	$I_{YY}$	0	torsional area moment of inertia	
11	$I_{ZZ}$	100	bending area moment of inertia about z-axis	
Connection element on the left wing				19
12	$I_{XX}$	0	bending area moment of inertia about x-axis	
13	$I_{YY}$	0	torsional area moment of inertia	
14	$I_{ZZ}$	30.8	bending area moment of inertia about z-axis	
Vertical tail				39 - 41
15	$I_{XX}$	0.2	bending area moment of inertia about x-axis	
16	$I_{ZZ}$	42.1	torsional area moment of inertia	
Connection element on the vertical tail				42
17	$I_{XX}$	11.1	bending area moment of inertia about x-axis	
18	$I_{ZZ}$	0.1	torsional area moment of inertia	
Connection elements on the horizontal tailplane				34 - 35
19	$I_{XX}$	0.1	bending area moment of inertia about x-axis	
20	$I_{YY}$	0	torsional area moment of inertia	
Fuselage/wings connection element				44
21	$I_{ZZ}$	78.8	torsional area moment of inertia	
Fuselage/tail connection element				43
22	$I_{ZZ}$	0.1	torsional area moment of inertia	

## CONCLUSION

This paper has reported preliminary results obtained on the GARTEUR SM-AG19 structure proposed as benchmark in the framework of COST Action F3 in structural dynamics. A F.E. beam model of very low order was generated to represent experimental data in the active frequency range from 0 to 65 Hz. It was shown that this model was able to predict structural modifications but was not convenient to reproduce modal data with accuracy in the passive frequency range (beyond 65 Hz). In order to improve the model, the objective function used for model updating should be extended to the full set of modes and new updating parameters should probably be chosen (tip masses, densities, etc). Further work will consider a higher order model using shell elements.



Table 3: Resonance frequency deviations

(a) Initial model					(b) Updated model				
Mode n°	Exp. Hz	F.E. Hz	MAC	$ df/f $ %	Mode n°	Exp. Hz	F.E. Hz	MAC	$ df/f $ %
1	6.5480	5.9080	0.9798	-9.7740	1	6.5480	6.2120	0.9799	-5.1313
2	16.6100	15.9400	0.9542	-4.0337	2	16.6100	16.6100	0.9558	0
3	34.8800	31.4100	0.6878	-9.9484	3	34.8800	34.9900	0.9634	0.3154
4	35.3600	31.4500	0.6952	-11.0577	4	35.3600	35.3100	0.9482	-0.1414
5	36.7100	35.4300	0.7991	-3.4868	5	36.7100	36.3600	0.9413	-0.9534
6	50.0900	47.8400	0.9662	-4.4919	6	50.0900	50.2900	0.9662	0.3993
7	50.7200	46.4700	0.9548	-8.3793	7	50.7200	50.6900	0.9467	-0.0591
8	56.4400	57.0200	0.9921	1.0276	8	56.4400	57.7000	0.9889	2.2325
9	65.1400	61.9800	0.8843	-4.8511	9	65.1400	64.5300	0.9069	-0.9364
			<b>0.8793</b>	<b>6.3389</b>				<b>0.9553</b>	<b>1.1299</b>
10	69.6400	59.7300	0.9709	-14.2303	10	69.6400	70.3100	0.9702	0.9621
11	105.5000	96.4100	0.9838	-8.6161	11	105.5000	97.8400	0.9850	-7.2607
12	134.3000	96.4100	0.7755	-28.2130	12	134.3000	97.8400	0.7765	-27.1482
13	134.7000	122.7000	0.7946	-8.9087	13	134.7000	124.1000	0.7718	-7.8693
14	139.3000	200.5000	0.0191	43.9340	14	139.3000	228.3000	0.3963	63.8909

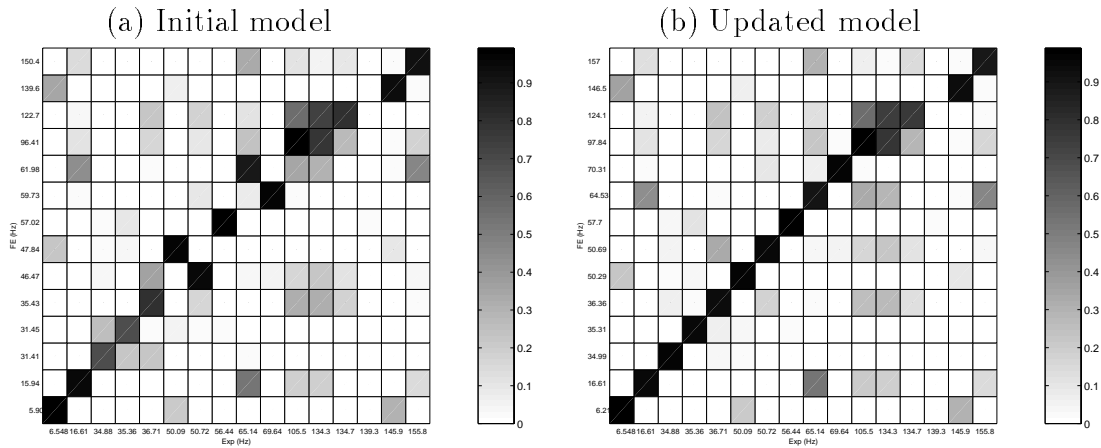


Fig. 4: MAC matrices between the analytical and experimental modes

## REFERENCES

- [1] Collignon P., Golinval J.C., "Finite Element Model Updating and Failure Detection based on Constitutive Equation Errors ", 2nd International Conference in Structural Dynamics Modelling : Test, Analysis, Correlation & Updating, Proceedings of the DTA/NAFEMS Conference held in Lake Windermere, Cumbria, UK, 3-5 July 1996, pp. 307-317.
- [2] Pascual R., "Model Based Structural Damage Assessment Using Vibration Measurements ", Ph. D. Thesis, University of Liège, Belgium, 1999.
- [3] Fraeijns de Veubeke, "Displacement and Equilibrium Models in Finite Element Method ", Stress Analysis, Ed. Zienkiewicz, John Wiley, 1965, Chap 9.
- [4] O'Callahan J., Avitabile P., "System Equivalent Reduction Expansion Process (SEREP) ", Proceedings of the 7th IMAC, Las Vegas, Nevada, 1989, pp. 29-37.

Table 4: Resonance frequency deviations (Structural modifications)

(a) Modification n° 1

Mode n°	Exp. Hz	F.E. Hz	MAC	$ df/f $ %
1	6.5410	6.2100	0.9963	-5.0604
2	13.9400	13.7500	0.9864	-1.3630
3	32.3600	30.5200	0.9729	-5.6860
4	35.0900	35.0800	0.7712	-0.0285
5	35.5200	35.4000	0.9914	-0.3378
6	38.1000	38.4600	0.9798	0.9449
7	48.6800	47.6300	0.8875	-2.1569
8	50.1700	50.3000	0.9876	0.2591
9	56.4600	57.8400	0.6586	2.4442
			<b>0.9146</b>	<b>2.0312</b>
10	58.1600	57.0100	0.8460	-1.9773
11	78.5100	75.1600	0.9218	-4.2670

(b) Modification n° 2

Mode n°	Exp. Hz	F.E. Hz	MAC	$ df/f $ %
1	6.3080	5.9380	0.4862	-5.8656
2	16.4300	16.4000	0.9308	-0.1826
3	27.2800	28.1400	0.9655	3.1525
4	35.3600	35.2800	0.9176	-0.2262
5	36.4600	36.1800	0.8870	-0.7680
6	48.9200	48.8700	0.9090	-0.1022
7	50.0100	50.0800	0.9551	0.1400
8	54.3400	55.5300	0.9736	2.1899
9	64.5400	63.6900	0.9127	-1.3170
			<b>0.8819</b>	<b>1.5493</b>
10	69.5500	70.2900	0.9536	1.0640
11	105.1000	97.2100	0.8987	-7.5071
12	134.1000	124.0000	0.9445	-7.5317
13	144.3000	144.2000	0.9017	-0.0693
14	155.8000	155.9000	0.8813	0.0642

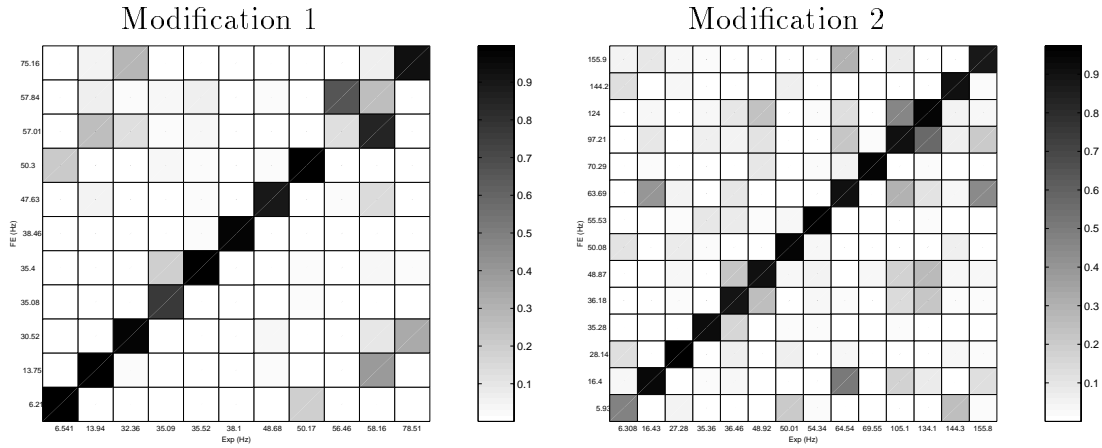


Fig. 5: MAC matrices between the analytical and experimental modes of the modified structures

[5] Degener M, Hermes M., "Ground Vibration Test and Finite Element Analysis of the GARTEUR SM-AG19 Testbed ", Deutsche Forschungsanstalt für Luft- und Raumfahrt e. V., Institut für Aeroelastik (23200), October 1996.

[6] SAMCEF v8.1-2 & BOSS-QUATTRO v2.1, ©Samtech s.a.